Effect of Nb doping on sintering and dielectric properties of PZT ceramics

Ali Mirzaei[1,*], Maryam Bonyani[1], Shahab Torkian[2]

[1]*Department of Materials Science and Engineering, Shiraz University, Shiraz, Iran*
[2]*Materials Engineering Department, Malek Ashtar University of Technology, Shahin Shahr, Iran*

Abstract

The extensive use of piezoelectric ceramics such as lead zirconate titanate (PZT) in different applications became possible with the development of donor or acceptor dopants. Therefore, studies on the effect of dopants on the properties of PZT ceramics are highly demanded. In this study undoped and 2.4 mol% Nb-doped PZT (PZTN) powders were successfully obtained by a solid-state reaction and calcination at 850 °C for 2 h. Crystallinity and phase formation of the prepared powders were studied using X-ray diffraction (XRD). In order to study morphology of powders, scanning electron microscopy (SEM) was performed. The crystalline PZT and Nb-doped PZT powders were pelleted into discs and sintered at 1100, 1150 and 1200 °C, with a heating rate of 10 °C/min, and holding time of 1–6 h to find the optimum combination of temperature and time to produce high density ceramics. Microstructural characterization was conducted on the fractured ceramic surfaces using SEM. Density measurements showed that maximal density of 95% of the theoretical density was achieved after sintering of PZT and PZTN ceramics at 1200 °C for 2 h and 4 h, respectively. However, the results of dielectric measurements showed that PZTN ceramics have higher relative permittivity (ε_r ~17960) with lower Curie temperature (~358 °C) relative to PZT (ε_r = 16000 at ~363 °C) as a result of fine PZTN structure as well as presence of vacancies. In addition, dielectric loss (at 1 kHz) of PZT and PZTN ceramics with 95% theoretical density was 0.0087 and 0.02, respectively. The higher dielectric loss in PZTN was due to easier domain wall motions in PZTN ceramics.

Keywords: PZT, Nb_2O_5 doping, powder synthesis, sintering, microstructure, permittivity

I. Introduction

Lead zirconate titanate (PZT) has perovskite structure with general formula of ABO_3. When Zr:Ti ratio is smaller than 95:5 all of compositions are ferroelectric at room temperature [1]. Above the Curie temperature, its unit cell is cubic, but below of the Curie temperature, it is distorted to either tetragonal (Zr:Ti < 53:47) or rhombohedral (Zr:Ti > 53:47). The boundary between these two phases (Zr:Ti ~ 53:47 at RT) is known as the morphotropic phase boundary (MPB). In the 1950s, it was discovered that PZT ceramics with a Zr:Ti ratio approximately 52:48 have excellent properties, such as high Curie temperature, high electromechanical coupling coefficient, easy poling and doping, and high dielectric, ferroelectric and piezoelectric properties [2,3]. It was shown that the coexistence of tetragonal and rhombohedral phases is responsible for the excellent properties of PZT ceramics [4–6]. Due to exceptional properties, PZT ceramics are used in numerous applications, such as phonograph pickups, air transducers, underwater sound and ultrasonic generators, delay line transducers, wave filters, etc. [7,8]. For these applications, high dielectric constant and good ferroelectric properties, such as low coercive field (E_c), high remnant polarization (P_r) and high dielectric constant (ε_r) are desired. These properties can be tuned by doping PZT ceramics with donor dopants like Nb^{5+}, Sb^{5+} and Ta^{5+}, or acceptor dopants such as La^{3+}. Furthermore, the electrical properties of PZT ceramics can be tuned towards hard or soft characteristics by means of proper doping [9]. The terms "soft" and "hard" PZT ceramics refer to the mobility of the dipoles or domains, as well as to the polarization and depolarization behaviour [10]. The

*Corresponding author: tel: +98 71 3721 1984,
fax: +98 71 3721 1984, e-mail: alisonmirzaee@yahoo.com*

soft PZT ceramics are obtained by doping with donor dopants, such as W^{6+} (for site A) and Nb^{5+}, Sb^{5+} (for site B), leading to the creation of vacancies on "A" site in the lattice. High domain wall mobility and resulting soft ferroelectric behaviour are characteristics of these doped ceramics. These features lead to large piezoelectric charge coefficient, moderate permittivity and high coupling factors which make them interesting for actuators, sensors, ultrasonic transmitters and receivers for flow or level measurement [11,12].

The main drawback of the pure PZT material for high advanced applications is the poor dielectric, ferroelectric and piezoelectric properties due to limited domain movement [3]. In most cases, high-performance PZT ceramics with enhanced dielectric, piezoelectric and ferroelectric properties can be obtained using donor dopants such as Nb^{5+} [13]. Although the effect of Nb^{5+} doping in PZT thin films is extensively studied [13–15], there are only a few papers about Nb^{5+} doping in bulk (PZTN) ceramics [16,17], which are mostly focused on piezoelectric properties. The present work concerns the synthesis of PZT and PZTN powders via solid-state reaction and investigation of sintering behaviour and dielectric properties.

II. Experimental procedure

2.1. Solid-state synthesis

PbO (Merck 99%), TiO_2 (rutile, Aldrich 99.8%), ZrO_2, (Aldrich 99%) and Nb_2O_5 (Merck 99.5%) were used as starting materials without further purification. The precursor oxides were weighed according to desired stoichiometry of the final products, i.e. the pure PZT ($Pb(Zr_{0.52}Ti_{0.48})O_3$) and 2.4 mol% Nb_2O_5 doped PZT ($Pb(Zr_{0.52}Ti_{0.48})_{0.976}Nb_{0.024}O_3$) powders. Then the powders were put into a jar containing zirconia balls and isopropanol as milling medium. After the wet milling for 24 h, dry powders were obtained by evaporation of isopropanol at 85 °C for 2 h. The dried powders were ground in an agate mortar and finally calcined at 850 °C for 2 h to obtain desired perovskite phase (Fig. 1). Calcination was done in the zirconia crucibles with heating rate of 5 °C/min. During cooling step, when the temperature of furnace reached 350 °C (estimated Curie temperature), the powders were air quenched. In order to obtain a homogeneous distribution of particles and breaking of big agglomerates formed during calcination, the second stage of ball milling was done for 12 h. Finally, a high energy ball milling was performed on the powders for 4 h to further downsize the particles. The parameters of ball milling and high energy milling are presented in Table 1.

2.2. Shaping and sintering

The prepared PZT and PZTN powders calcined at 850 °C were used for preparation of ceramic discs. The powders were mixed with 5 wt.% of a water solution containing 10% polyvinyl alcohol (PVA) and pressed into discs with 10 mm in diameter and 1–2 mm in thickness in stainless steel dies under uniaxial pressure of 150 MPa. The pressed discs were placed in a covered alumina crucible where atmosphere was controlled by the addition of the pure PZT (52/48) + 10% ZrO_2 powders in the crucible without contact with the samples (Fig. 1). The discs were sintered at 1100, 1150 and 1200 °C for 1–6 h, with 4 h holding at 550 °C to burn-out the binder. The initial heating rate was set to be 5 °C/min up to the burn-out temperature and then a heating rate of 10 °C/min was used up to the final sintering temperature.
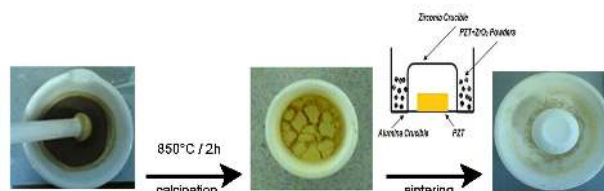

Figure 1. As-prepared and calcined PZT powders and sintered PZT sample (with set-up used for sintering)

Table 1. Parameters of ball milling and high energy milling

Parameter	Ball milling	High energy milling
Diameter of balls	10 mm	1 mm
RPM	100	300
Powders to balls weight ratio	1:10	1:15
Powders to isopropanol weight ratio	1:1	1:1

2.3. Characterization

The phase formation of the powders and sintered bodies was examined by X-ray diffractometer (Brucker, Germany) using CuKα radiation (λ = 1.5418 Å). The XRD patterns were recorded at room temperature at a scan rate 0.05°/s. Particle size distribution was measured using a laser particle size analyser (Horiba, LB-550, Japan), dispersing a small amounts of the powder in water and left in an ultrasonic bath before measurements. Microstructure characterization was conducted on the fractured sample surfaces by scanning electron microscopy (SEM, Cambridge, UK). The density of the sintered samples was determined by the Archimedes method using distilled water.

2.4. Dielectric measurements

The relative permittivity and dielectric loss ($\tan\delta$) were evaluated from capacitance measured on a HP 4284A LCR meter at a frequency of 1 kHz and as a function of temperature. The LCR meter was used in conjunction with a computer-controlled temperature chamber. Capacitance was converted to relative permittivity using the sample geometry and permittivity of air.
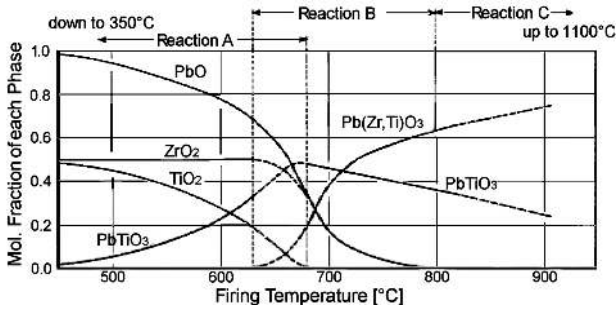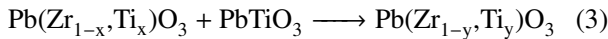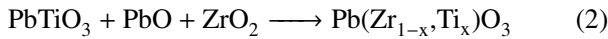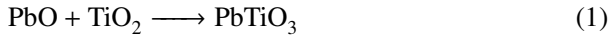
Figure 2. Phases in PbO-ZrO$_2$-TiO$_2$ system as a function of temperature [18]

III. Results and discussion

3.1. Characterization of PZT and PZTN powders

PZT formation mechanism during calcination process is shown in Fig. 2. PZT is formed as a result of three sequential reactions [18]:

$$PbO + TiO_2 \longrightarrow PbTiO_3 \tag{1}$$

$$PbTiO_3 + PbO + ZrO_2 \longrightarrow Pb(Zr_{1-x},Ti_x)O_3 \tag{2}$$

$$Pb(Zr_{1-x},Ti_x)O_3 + PbTiO_3 \longrightarrow Pb(Zr_{1-y},Ti_y)O_3 \tag{3}$$

In the first reaction that occurs between 350–680 °C, PbO diffuses into TiO$_2$. In this stage amounts of PbO and TiO$_2$ gradually decrease and a new phase, i.e. PbTiO$_3$ phase is formed, while the amount of ZrO$_2$ is constant. In the second reaction, which occurs between 620–800 °C, amount of PbTiO$_3$ phase decreases and Pb(Zr$_{1-x}$,Ti$_x$)O$_3$ (PZT) as a new phase is formed. With increase of temperature the amount of this phase increases. At the end of this stage, PbO, TiO$_2$ and ZrO$_2$ totally disappear. In the third reaction which starts at 800 °C, amount of Pb(Zr$_{1-x}$,Ti$_x$)O$_3$ phase increases, while PbTiO$_3$ phase decreases.

During calcination of PZT powders usually two crystalline structures are observed. The first one is a stable and desired structure with excellent electrical properties, i.e. perovskite with general formula ABO$_3$ (Pb(Zr$_{1-x}$Ti$_x$)O$_3$). The second one is a metastable and undesired structure, i.e. pyrochlore phase with poor electrical properties due to large defect density as a result of oxygen or lead deficiency, with general formula A$_2$B$_2$O$_{7-x}$ (Pb$_2$(Zr$_{1-x}$Ti$_x$)$_2$O$_{7-x}$) [19]. As the main purpose of calcination process is to reach desired perovskite structure, it is essential to avoid formation of pyrochlore structure during calcination process.

Figures 3a and 3b show XRD patterns of the calcined PZT and PZTN powders, respectively. All peaks can be indexed as perovskite PZT structure. If PbO is added in excess (above the stoichiometry), in addition to perovskite, another phase will be formed due to impossibility of vacancy creation in B site [2]. Thus, the presence of only perovskite structure in the calcined powders (Fig. 3a,b) confirms good design of the used synthesis and calcination processes. Figures 3c and 3d show enlarged XRD patterns (2θ = 42.5–46.5°) of PZT and PZTN powders, respectively. Coexistence of tetra-
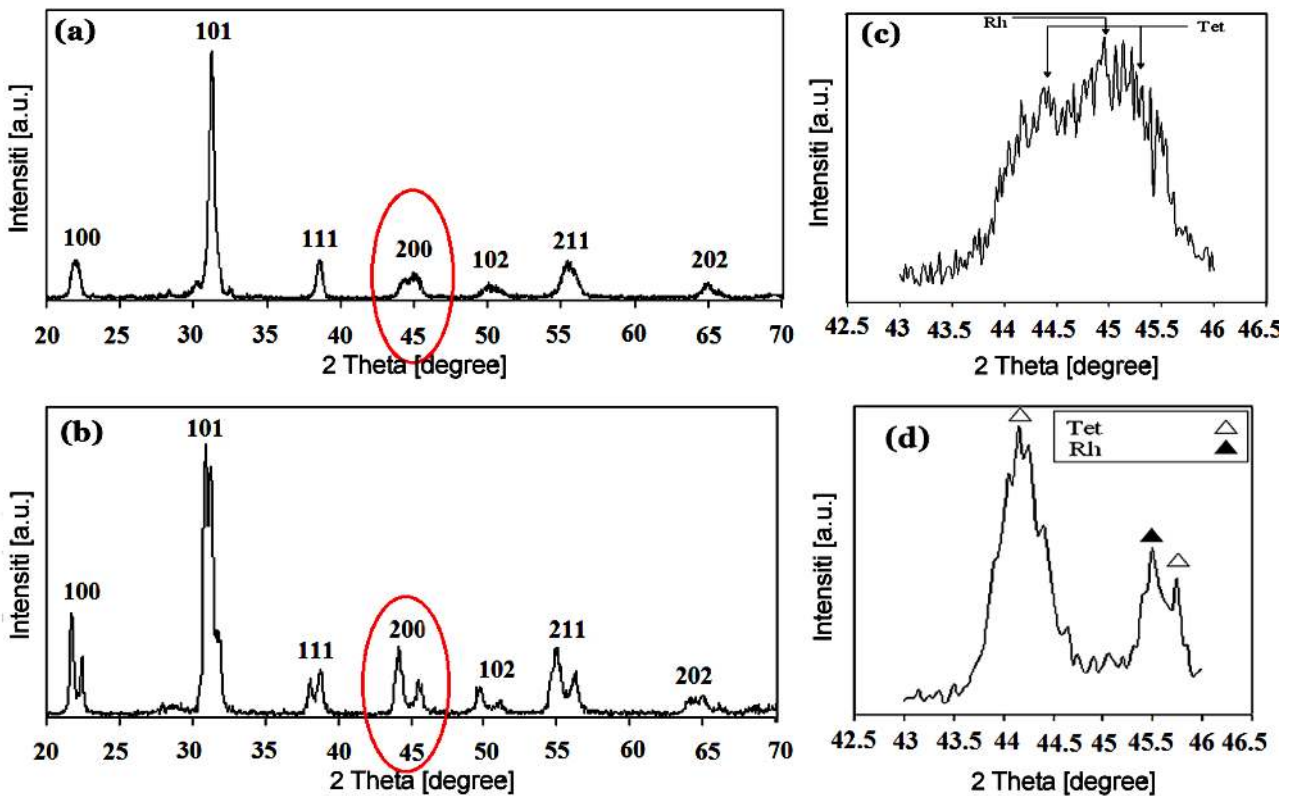

Figure 3. XRD pattern of: a) PZT and b) PZTN powders calcined at 850 °C/2 h and corresponding enlarged XRD patterns (2θ = 42.5–46.5°) – (c) and (d) respectively
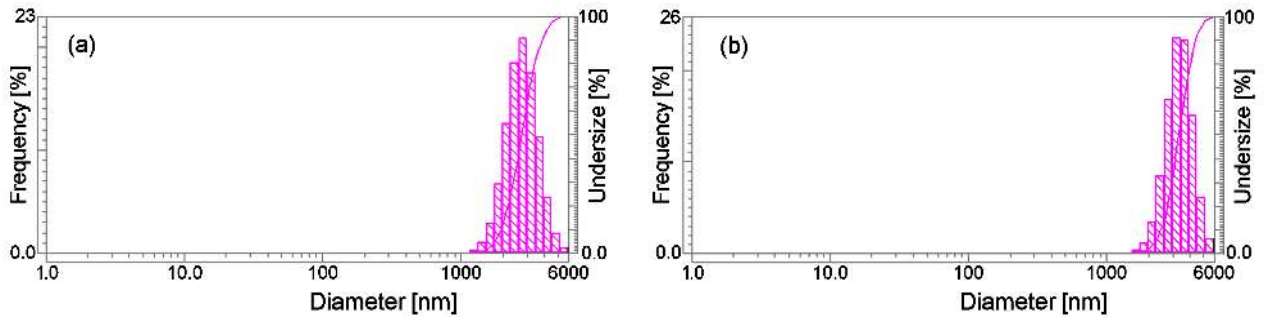
Figure 4. Particle size distribution of: a) PZT and b) PZTN powders prepared by solid-state reaction and calcined at 850 °C for 2 h, after high energy ball milling
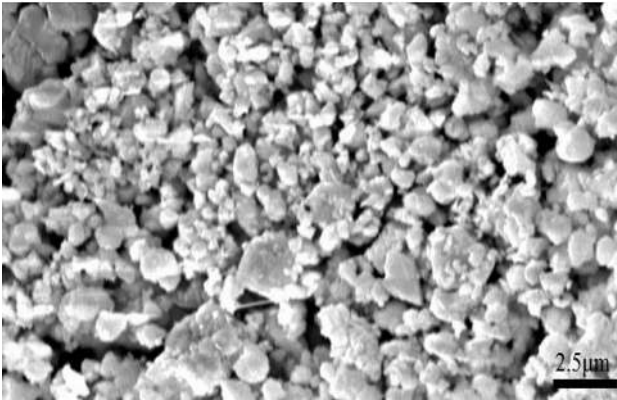

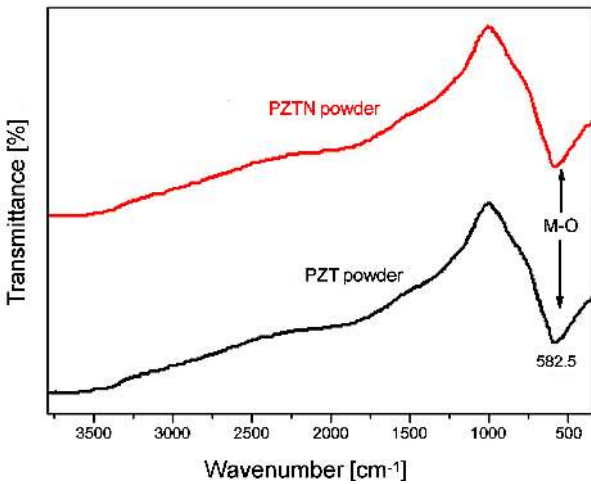**Figure 5. SEM micrograph of PZTN powders calcined at 850 °C for 2 h**

Figure 6. FTIR spectra of PZT and PZTN powders calcined at 850 °C for 2 h

gonal and rhombohedral phases in perovskite structure of PZT is clearly observed (Fig. 3c). In fact, due to inhomogeneity of chemical composition resulted from solid-state reaction, tetrahedral and rhombohedral phases are distinguishable. The clear separation between tetrahedral and rhombohedral phases in PZTN discs (Fig. 3d) can be attributed to the presence of Nb^{5+} in the structure that causes more inhomogeneity of chemical composition within the grains [20].

Figures 4a and 4b show particle size distribution of the PZT and PZTN powders calcined at 850 °C for 2 h

followed by high energy ball milling, respectively. A salient feature of these powders is that they have relatively narrow distribution and the mean particle size approximately in the range 3–4 μm.

Figure 5 shows SEM micrograph of PZTN powders after calcination at 850 °C for 2 h. As it can be seen, the powders have relatively narrow distribution with average particle size about 3–3.5 μm, which is in agreement with PSA results.

Figure 6 shows FTIR spectra of PZT and PZTN powders after calcination at 850 °C for 2 h. A sharp band at 582.5 cm^{-1} was formed and can be attributed to the M–O bonding (M = Ti, Zr, Nb and Pb) [21]. The O–H peaks are not observed in FTIR spectra of these powders due to high calcination temperature. There is no significant difference between FTIR spectra of PZT and PZTN powders, because Nb^{5+} ions replace Ti^{4+}/Zr^{4+} ions and make Nb–O bonds with FTIR peak at 585.5 cm^{-1} (similar to the positions of Ti–O or Zr–O bonds).

3.2. Sintering behaviour of PZT and PZTN ceramics

There are several reasons why a high density ferroelectric ceramics are required in most applications. Firstly, dielectric constant of ferroelectric ceramics increases with increasing density, because the relative dielectric constant of pores/vacuum is unit. Secondly, the presence of pores generally causes high dielectric loss,
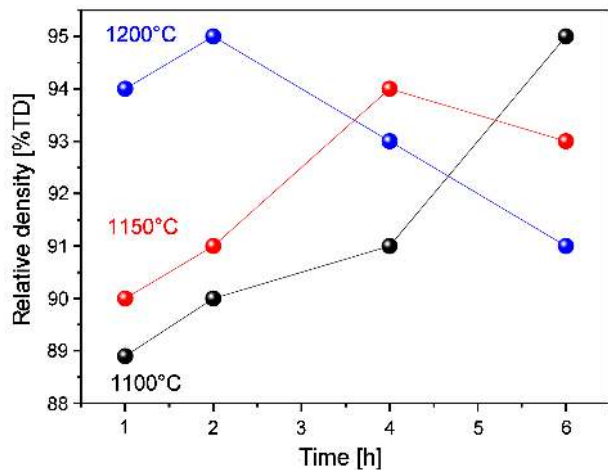

Figure 7. Density of PZT discs prepared by solid-state reaction as a function of sintering temperature and time

since porosity could provide conduction path for electricity. Moreover, mechanical strength is directly determined by density of a material. Finally, electrical conduction caused by porosity is also responsible for degraded electrical breakdown strength [22].

Figure 7 shows density of PZT discs as a function of temperature and time. PZT discs sintered at 1100 °C for 2 h had relative density of 88 %TD (theoretical density) which continuously increased with sintering time. Thus, relative density of 95 %TD was reached after sintering at 1100 °C for 6 h. At 1150 °C, with increase of time to 4 h there is obvious increase of density (Fig. 7), due to the increase of diffusion rate and improvement of sintering process. However, with further increase of time to 6 h, density drops due to evaporation of lead oxide, grain growth and presence of pores insides the grains (Fig. 8) [23]. At 1200 °C, optimum sintering time was 2 h, which was enough to reach 95 %TD. With further increases of time to 4 h or 6 h, due to vaporization of PbO and grain growth (Fig. 9), it was impossible to reach higher densities.

In order to improve electrical properties of PZT ceramics and grain growth inhibition during sintering, PZT ceramics with 2.4 mol% Nb_2O_5 were prepared. Due to presence of small interstitial sites in the perovskite structure (Fig. 10) and ionic radius of Nb^{5+} (0.78 Å), Zr^{4+} (0.86 Å), Ti^{4+} (0.745 Å) and Pb^{2+} (0.133 Å) [25], it is expected that Nb^{5+} substitutes Zr^{4+} and Ti^{4+} on B-site in perovskite structure. However, when a doped ions are added in perovskite structure, electrical neutrality must always remain unchanged. Thus, by the substitution of Nb^{5+} ion on B-site, additional positive charge is introduced and Pb^{2+} vacancies are created to maintain charge neutrality, leading to formation of soft PZT. For every two Nb^{5+} ions introduced into the lattice, one Pb^{2+} vacancy is formed. This vacancy pair can align itself with polarization of PZT and due to the increased mobility of domain walls, could improve permittivity of PZTN.

Figure 11 presents density of PZTN ceramics as a function of temperature and time. As it can be seen, sintering temperature of 1150 °C is not sufficient to reach a high value of density as the obtained highest density was ~90 %TD. Therefore, the PZTN ceramics were sintered at 1200 °C and 93 %TD and 95 %TD were obtained after 2 h and 4 h, respectively (Fig. 11). That is the maximum density for PZTN ceramics. Incorporation of Nb^{5+} into structure of PZT causes formation of Pb vacancies and improved diffusion and final density. However, created Pb vacancies as a result of Nb^{5+} addition have electrical charge and low mobility [26]. Therefore, these samples need higher sintering temperature or longer sintering time than the pure PZT. In fact high density of PZTN ceramics is principally due to grain growth inhibition (Fig. 12) [25]. Nb^{5+} ions precipitate near grain boundaries and lead to significant reduction of their movement. When boundary moves, it must take precipitated ions with itself. This causes decrease of
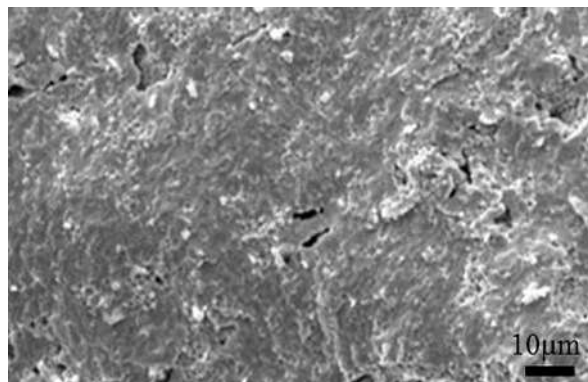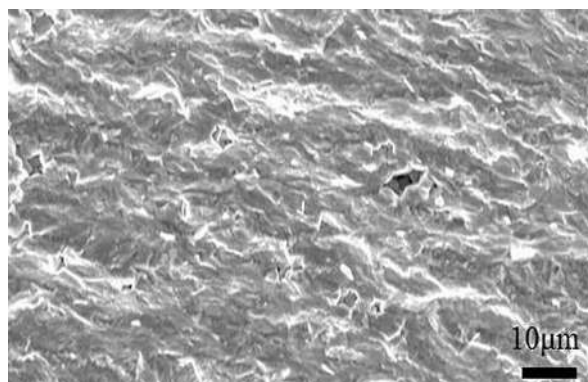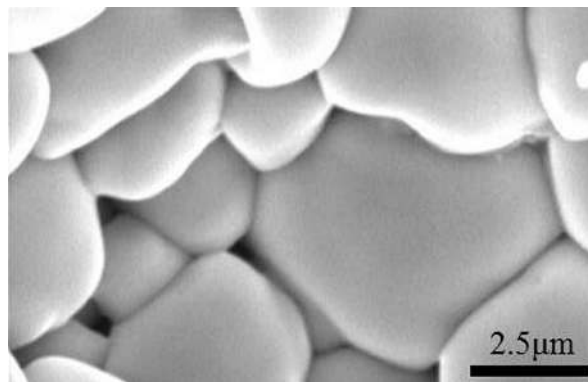

Figure 8. SEM micrograph of PZT ceramics sintered at 1150 °C for 6 h

(a)

(b)

Figure 9. SEM micrographs of fracture surface of PZT discs calcined at 1200 °C for: a) 2 h and b) 6 h
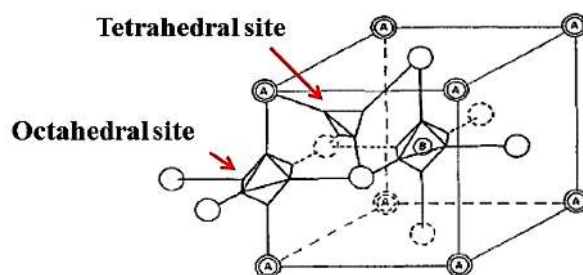

Figure 10. Tetrahedral and octahedral sites in perovskite structure [24]
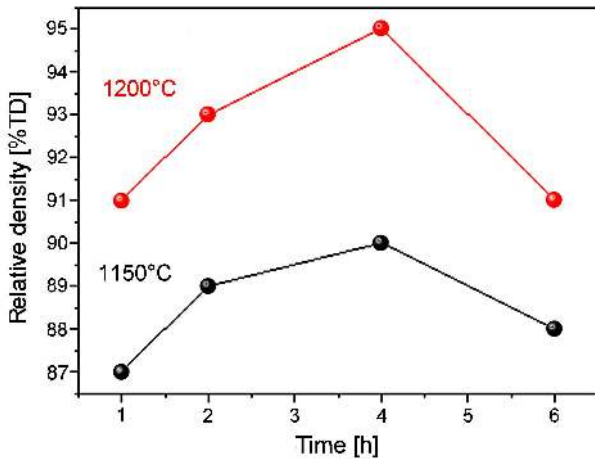
Figure 11. Density of PZTN ceramics as a function of sintering temperature and time

grain boundary mobility and eventually creation of fine grain structure and improvement of electrical properties of PZTN ceramics [24].

Figures 13a and 13b show the XRD patterns of PZT and PZTN ceramic discs after sintering at 1200 °C for 2 and 4 h, respectively. Compared with XRD patterns of PZT and PZTN powders (Fig. 2), no additional phase is formed. Furthermore, the peaks are sharper, indicating grain growth during sintering at high temperature. Figures 13c and 13d show enlarged XRD patterns of the circled area in corresponding XRD patterns. It can be seen that splitting of tetragonal and rhombohedral phases is decreased which can confirm better chemical homogeneity in the sample sintered at high temperatures.

A serious problem in preparation PZT ceramics is preserving the desired composition due to the fact that the evaporation of lead oxide leads to change of the stoichiometry. The weight of the samples before and after sintering was measured by a sensitive balance and the difference between these two values was reported as mass loss after sintering. Mass losses after sintering at

1150 °C for 4 h are 3.4% and 3% for PZT and PZTN ceramics, respectively. Somewhat higher mass losses were observed at 1200 °C for 4 h, i.e. 4% and 3.5% for PZT and PZTN ceramics, respectively. In the present case, the mass loss, related to the volatilization of lead oxide and PVA used as binder, is higher for the pure PZT than for PZTN ceramics. In the case of PZTN, the main factor that controls PbO evaporation is the penetration of Nb^{5+} ions in perovskite structure. It was previously reported [27] that dopants hinder the evaporation of the lead oxides. This can explain the relatively smaller mass loss of PZTN in comparison with the pure PZT ceramics.

3.3. Dielectric properties

Figure 14 shows variations of relative permittivity of PZT and PZTN ceramics (sintered at 1200 °C for 2 and 4 h, respectively) as a function of temperature. As it can be seen, upon doping with 2.4 mol% Nb^{5+} Curie temperature of PZTN ceramics is lower for about 5 °C and relative permittivity is higher in comparison to the pure PZT samples. Thus, room temperature relative permittivity of PZTN is 1178, while that for PZT is 925. Also, maximum relative permittivity of PZT is ~16000 and that for PZTN is ~17960. Higher relative permittivity and lower Curie temperature in PZTN ceramics are due to the fact that domain wall motion becomes easier with donor dopant such as Nb^{5+}. In fact due to presence of vacancies in PZTN ceramics, domain walls move easier and align themselves by external electric field, resulting in better polarization and consequently higher dielectric constant [28].

Relationship between dielectric permittivity and the temperature above Curie temperature is described by Curie-Weiss law [29]:

$$\varepsilon_r = \varepsilon_0 + \frac{C}{T - T_0} \tag{4}$$

where ε_0 is permittivity of vacuum (8.854×10^{-12} F/m), C is Curie-Weiss constant, T_0 is Curie point (Curie tem-
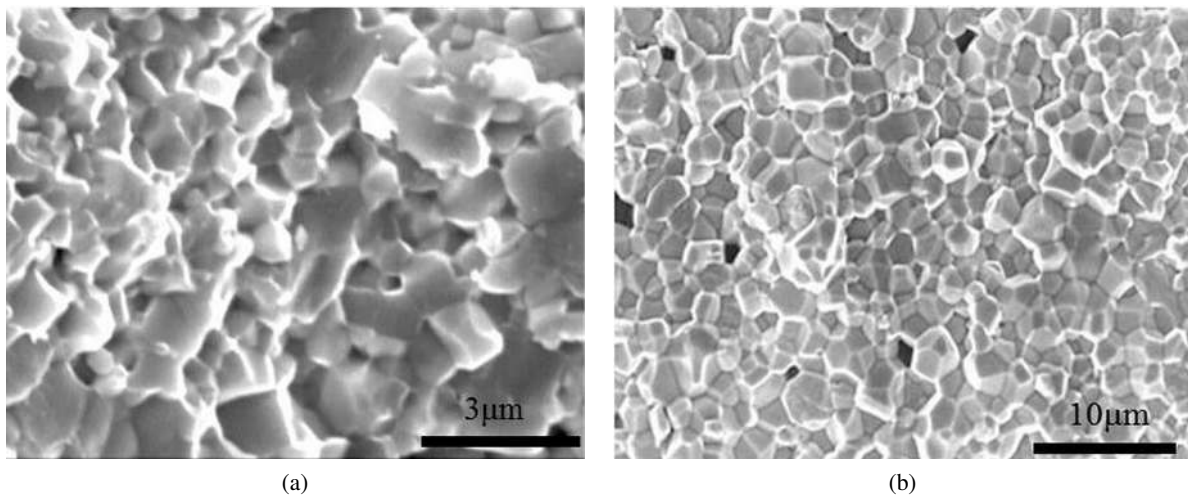

(a)

(b)

Figure 12. SEM micrographs of fracture surface of PZTN ceramics after sintering at 1200 °C for: a) 2 h and b) 4 h
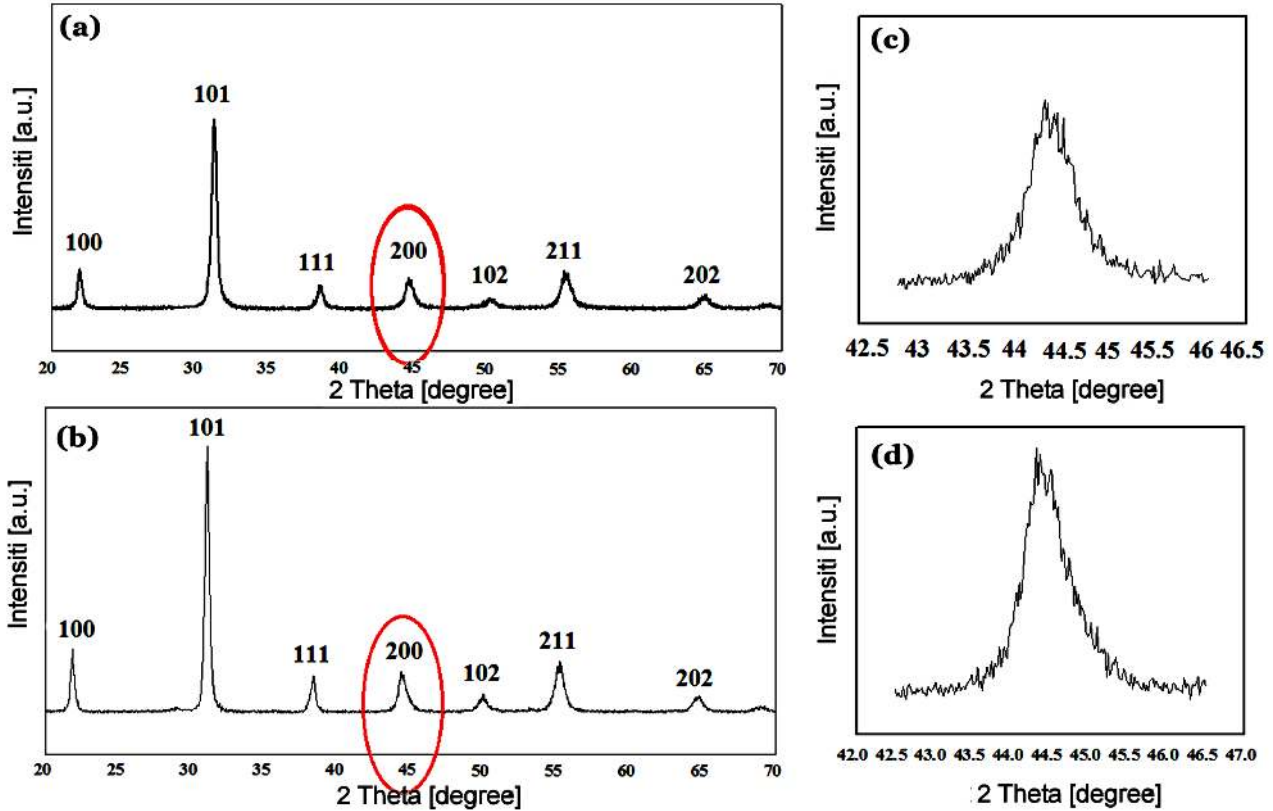
Figure 13. XRD pattern of: a) PZT discs sintered at 1200 °C for 2 h, b) PZTN discs sintered at 1200 °C for 4 h and corresponding enlarged XRD patterns (2θ = 42.5–46.5°) – (c) and (d) respectively

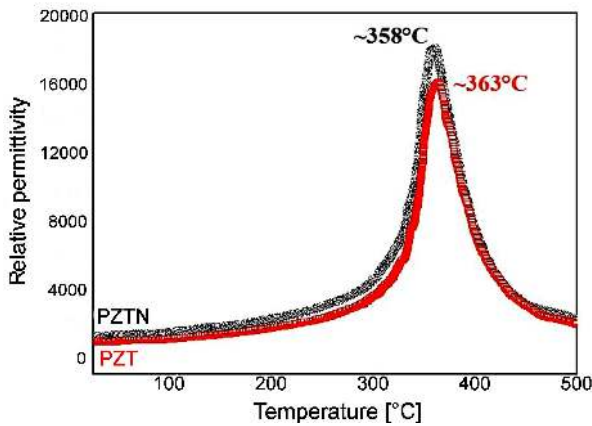**Figure 14. Relative permittivity of PZT and PZTN ceramic discs as a function of temperature at 1 kHz**

perature is about 10 °C lower than Curie point) and T is temperature. According to above equation, with increase of temperature above Curie point, the permittivity drops gradually. The same trend was observed for PZT and PZTN ceramics, where the permittivity of both materials decreases upon increase of the temperature above their corresponding Curie temperature.

Dielectric loss (at 1 kHz) for both PZT and PZTN ceramics were obtained. Dielectric loss at 1 kHz and room temperature for PZT and PZTN ceramics with 95 %TD was 0.0087 and 0.02, respectively. It is accepted that for ferroelectric ceramics whole dielectric loss is due to do-

main wall motion. In PZTN ceramics owing to the presence of vacancies, domain walls can move more easily, therefore even under the small electrical field, domain walls move resulting in higher dielectric loss.

IV. Conclusions

In this study undoped PZT and 2.4 mol% Nb-doped PZT powders (PZTN) were successfully synthesized by solid-state reaction and calcined at 850 °C for 2 h. The calcined powders have perovskite structure with mixture of tetrahedral and rhombohedral phases and the average particle size of 3–4 μm. The optimal sintering conditions that produce ceramics with 95 %TD were found to be 1200 °C/2 h for PZT and 1200 °C/4 h for PZTN ceramics. The results of relative permittivity measurements indicate that PZTN ceramics had higher dielectric permittivity with lower Curie temperature as a result of fine structure as well as presence of vacancies. Also, dielectric losses (at 1 kHz) of PZTN ceramics were higher than PZT ceramics, due to easier movement of domain walls in PZTN ceramics.

References

1. T.K. Mandal, S. Ram, "Synthesis of $PbZr_{0.7}Ti_{0.3}O_3$ nanoparticles in a new tetragonal crystal structure

with a polymer precursor", *Mater. Lett.*, **57** (2003) 2432–2442.

2. B. Jaffe, W.R. Cook, H. Jaffe, *Piezoelectric Ceramics*, Academic Press, London, UK, 1971.

3. A. Rachakom, S. Jiansirisomboon, A. Watcharapasorn, "Physical and electrical properties of Nb doped $Bi_{0.5}Na_{0.5}[Zr_{0.59}Ti_{0.41}]O_3$", *Ceram. Int.*, **38** (2012) S385–389.

4. B. Jaffe, W.R. Cook, H. Jaffe, "Piezoelectric ceramics", *J. Sound Vib.*, **20** (1971) 562–563.

5. B. Noheda, D.E. Cox, "Bridging phases at the morphotropic boundaries of lead-oxide solid solutions", *Phase Transitions*, **79** (2006) 5–20.

6. M. Hinterstein, M. Hoelzel, J. Rouquette, J. Haines, J. Glaum, H. Kungl, M. Hoffman, "Interplay of strain mechanisms in morphotropic piezoceramics", *Acta Mater.*, **94** (2015) 319–327.

7. K. Uchino, *Ferroelectric Devices*, Marcel Dekker, USA, 2000.

8. L.M. Levinson, *Electronic Ceramics: Properties, Devices and Applications*, Marcel Dekker, USA, 1988.

9. M.I. Morozov, D. Damjanovic, "Charge migration in $Pb(Zr,Ti)O_3$ ceramics and its relation to ageing, hardening, and softening", *J. Appl. Phys.*, **107** (2010) 034106.

10. N. Horchidan, C.E. Ciomaga, R.C. Frunza, C. Capiani, C. Galassi, L.Mitoseriu, "A comparative study of hard/soft PZT-based ceramic composites", C*eram. Int.*, **42** (2016) 9125–9132.

11. P.S. Silva Jr., M. Venet, O. Florencio, "Influence of diffuse phase transition on the anelastic behavior of Nb-doped $Pb(Zr_{0.53}Ti_{0.47})O_3$ ceramics", *J. Alloys Compd.*, **647** (2015) 784–789.

12. M.M.S. Pojucan, M.C.C. Santos, F.R. Pereira, M.A.S. Pinheiro, M.C. Andrade, "Piezoelectric properties of pure and (Nb^{5+},Fe^{3+}) doped PZT ceramics", *Ceram. Int.*, **36** (2010) 1851–1855.

13. E.C.F. Souza, A.Z. Simoesa, M. Cilensea, E. Longoa, J.A. Varela, "The effect of Nb doping on ferroelectric properties of PZT thin films prepared from polymeric precursors", *Mater. Chem. Phys.*, **88** (2004) 155–159.

14. V. Kayasu, M. Ozenbas, "The effect of Nb doping on dielectric and ferroelectric properties of PZT thin films prepared by solution deposition", *J. Eur. Ceram. Soc.*, **29** (2009) 1157–1163.

15. T. Haccart, D. Remiens, E. Cattan, "Substitution of Nb doping on the structural, microstructural and electrical properties in PZT films", *Thin Solid Films*, **423** (2003) 235–242.

16. M. Pereira, A.G. Peixoto, M.J.M. Gomes, "Effect of Nb doping on the microstructural and electrical properties of the PZT ceramics", *J. Eur. Ceram. Soc.*, **21** (2001) 1353–1356.

17. S.Y. Chu, T.Y. Chen, I.T. Tsai, W. Water, "Doping effects of Nb additives on the piezoelectric and dielectric properties of PZT ceramics and its application on SAW device", *Sensors Actuators A: Phys.*, **113** (2004) 198–203.

18. Y. Matsuo, H. Sasaki, "Formation of lead zirconate-lead titanate solid solutions", *J. Am. Ceram. Soc.*, **48** (1965) 289–291.

19. A. Mirzaei, M. Bonyani, S. Torkian, "Synthesis and characterization of nanocrystalline PZT powders: From sol to dense ceramics", *Process. Appl. Ceram.*, **10** (2016) 9–16.

20. P. Amonpattaratkit, P. Jantaratana, S. Ananta, "Influences of PZT addition on phase formation and magnetic properties of perovskite $Pb(Fe_{0.5}Nb_{0.5})O_3$-based ceramics", *J. Magn. Magn. Mater.*, **389** (2015) 95–100.

21. T.I. Chang, J. Lhaung, H.P. Lin, S.C. Wang, H.H. Lu, L. Wu, J.F. Lin, "Effect of drying temperature on structure, phase formation, sol-gel derived lead zirconate titanate powders", *J. Alloys Compd.*, **414** (2006) 224–229.

22. P. Pramanik, R.N. Das, "Structure property relations of chemically synthesized nanocrystalline PZT powders", *Mater. Sci. Eng. A*, **304-306** (2001) 775–779.

23. M.N. Rahaman, *Ceramic Processing and Sintering*, CRC Press, New York, USA, 2003.

24. R.B. Atkin, R.M. Fulrath, "Point defects and sintering of lead zirconate titanate", *J. Am. Ceram. Soc.*, **54** (1971) 265–270.

25. M.W. Barsoum, *Fundamental of Ceramics*, IOP Publishing Ltd, USA, 2003.

26. M. Hammer, M.J. Hoffmann, "Sintering model for mixedoxide derived lead zirconate titanate ceramics", *J. Am. Ceram. Soc.*, **81** (1998) 3277–3284.

27. J.F. Fernández, C. Moure, M. Villegas, P. Durán, M. Kosec, G. Drazic, "Compositional fluctuations and properties of fine-grained acceptor-doped PZT ceramics", *J. Eur. Ceram. Soc.*, **18** (1998) 1695–1705.

28. C.H. Wang, S.J. Chang, P.C. Chang, "Effect of sintering conditions on characteristics of $PbTiO_3$-$PbZrO_3$-$Pb(Mg_{1/3}Nb_{2/3})O_3$-$Pb(Zn_{1/3}Nb_{2/3})O_3$", *Mater. Sci. Eng. B*, **111** (2004) 124–130.

29. Y. Guo, K.I. Kakimoto, H. Ohsato, "Dielectric and piezoelectric properties of lead-free ($Na_{0.5}K_{0.5}$)NbO_3-$SrTiO_3$ ceramics", *Solid State Commu.*, **129** (2004) 279–284.